Exhaust optimization for Viking Motorsports Formula SAE Team: Final Report - Spring 2016

Portland State University:

Maseeh College of Engineering and Computer Science

Team:		Sponsor:	PSU Advisor:
F. Vang	I. Prus	Viking Motorsports	Dr. Raul Cal Santiago
K. Marsh	K. Aghai	Contact: Franklin Vang	
A. Hupfeld	K. Cardin		
W. Al-Ibraheemi	L. Torres		

Table of Contents

Abstract

In an effort to demonstrate engineering principles and to apply engineering considerations to a product development, the VMS Exhaust capstone team sets out to redesign the Viking Motorsports Formula SAE (FSAE) combustion car exhaust system. With the current system failing to meet FSAE regulations and lacking in rigorous engineering design, the team is tasked with researching, designing, and manufacturing header and muffler components with consideration to noise attenuation, performance characteristics, and weight reduction. The final design includes dimensions for both header and muffler components as well as material selection and manufacturing methods. Testing concludes that the exhaust system meets FSAE regulations of 110 dB at max engine speed and 100 dB at idle. The new muffler also reduces weight by 2 lbs over the pre-existing system.

I. Introduction

Formula SAE dictates that all competition cars entering an event must pass a noise control test before being accepted into dynamic driving events. In 2015, Viking Motorsports struggled to pass the required limits of 110 dB at maximum engine speed and 100 dB at idle. Failure to pass the noise emission test would have resulted in disqualification from the event. The current capstone team is redesigning the complete exhaust system to ensure that the Formula SAE regulations are met and performance characteristics of the engine are conserved.

The current capstone team is designing and building a new exhaust system that will not exceed 110 dB at a maximum of 11250 rpm and 100 dB at idle speed, validated by use of a decibel reader oriented 45° from the horizontal and located 19.685 in. from the exhaust outlet. Secondary goals are to produce a system with a decrease in weight and increase in overall engine performance (*i.e.* horsepower and torque). Weight will be measured against the existing model and horsepower/torque data will be tested by use of a dynamometer with comparison to the existing design.

II. Exhaust

In order to characterize the flow and acoustic properties of a 4-stroke internal combustion (IC) engine it is necessary to understand the combustion process. The four unique processes in an ignition cycle of a 4-stroke engine are intake, compression, power, and exhaust. Figure 1 demonstrates the combustion cycle as (1) cylinder expansion for intake of air and fuel; (2) cylinder compression for proper pressure and temperature of air and fuel; (3) expansion of combusted gases post ignition for transfer of power to cylinder shaft; and (4) compression of cylinder to expel reacted gases out of the cylinders and into exhaust system.The frequency at which these processes are conducted along with the sudden release of gases following cycle (4)

generates acoustic noise that can meet or exceed levels of 100s of decibels. Additionally, the dynamics of the exhaust stroke can also affect the intake of air and fuel during valve overlap. During the exhaust stroke there is a period of approximately 10^{o} where both the intake and exhaust valves are open, providing an opportunity to actively pull the reacted gases out of the cylinder by control of the exhaust port pressure. The reacted gases are extracted from the cylinder if the pressure in the exhaust manifold is less than the pressure in the intake manifold; this phenomena is known as scavenging. The exhaust system, therefore, must account for both noise cancellation and performance design principles.

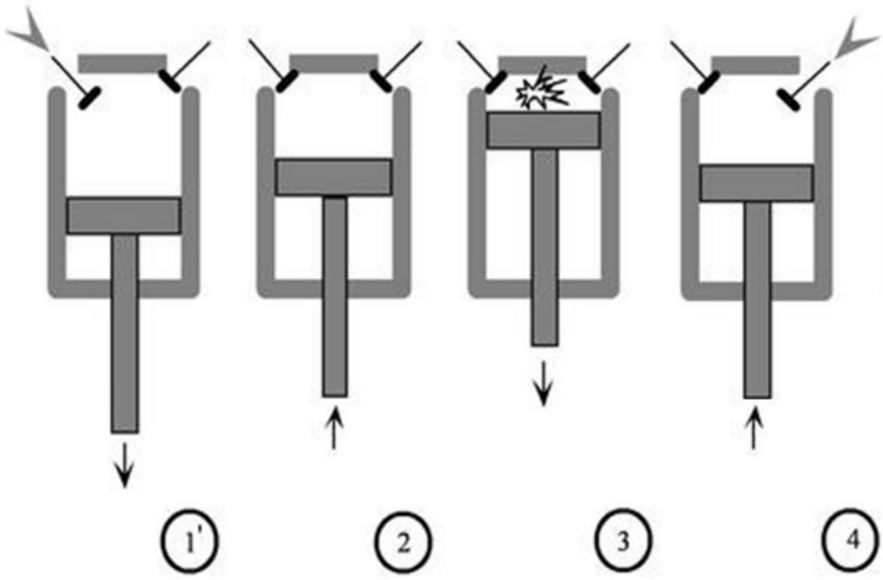

Figure 1. Four-stroke combustion cycle demonstrated as (1) intake, (2) compression, (3) combustion, and (4) expansion. Image adapted from Quattrochi (2006).

III. Header

Design of exhaust headers/manifolds involves evaluation of pipe diameter, length, and geometry. First to consider is header pipe diameter. At low engine speeds, high exhaust gas velocities are necessary to achieve quick throttle response. By means of conservation of mass, a small diameter exhaust pipe will result in higher gas velocity, conducive to throttle response for acceleration. However, without sufficient cross-sectional area, small diameter pipes may limit the mass flow rate needed to expel all combusted gases at higher rpm. Therefore, a compromise must be met to sufficiently provide high velocity flow with proper flow rate at peak engine speeds. Using tabulated data from Smith *et al.* (1972) which accounts for both gas velocity and

mass flow rate, a pipe diameter of 1.5 in. was found to provide sufficient flow for engine speeds up to 8,000 rpm.

Next to consider is the header length. For proper 'backpressure' or 'scavenging', as mentioned in sect. II, an ideal length is required to allow for reflected pressure waves to arrive back at the exhaust port in time for the valve overlap period. Changes in exhaust gas temperature throughout the engine revs results in a dynamic speed of sound, *c,* and therefore the optimum length can only be accounted for at one engine speed and its modes thereafter. Also, any change in geometry within the exhaust system will result in reflected pressure waves, and also significantly affect the length of the header pipes. Because of the complicated nature of the scavenging effects, literature reviews often provide guideline equations which are suited to a specific engine assuming an ideal straight exhaust pipe. Two equations by Smith *et al.* (1972) and Bell *et al.* (1988) give estimates lengths from cylinder characteristics and expected engine speeds and are given by

$$P = \frac{ASD^2}{1400d^2} \tag{1}$$

$$P = \frac{850(180+B)}{R} - 3 \tag{2}$$

where P represents pipe length in feet, A is exhaust open period in degrees, S is stroke length in inches, D is cylinder bore in inches, d is exhaust valve port diameter in inches, B is 180 plus the number of degrees the exhaust opens before BDC (bottom dead center), and R is the target rpm. Equations (1) and (2) result in a pipe length estimates of 18 in. and 21.24 in. respectively. The pipe length to the first collector was chosen to be 20inches. A final length to exhaust was chosen to be 10in, due to spatial constraints. A total description of header dimensions for diameter and length are given in Table 1 along with the main contributing reason for the decision.

Table 1. Design decisions for header component

Part	Dimension	Warrant
Primary to 2nd collector: Diameter	1.5"	Accepted Tabulated Data
Primary to 1st collector: Length	20"	Equations for Estimation
Primary to 2nd collector: Length	10"	Spatial Restrictions

Ideally the header pipes would be straight; however restrictions due to the amount of space between the car frame and the engine itself, as seen in Fig.2(left), require various bends and turns. In order to minimize the amount of sharp re-directions of the flow which can produce flow separation and recirculation zones, bends and curves were made at the largest allotted radii

given by space as well as the need to have equal lengths for all pipes. The final design can be seen in Fig. 2(right).

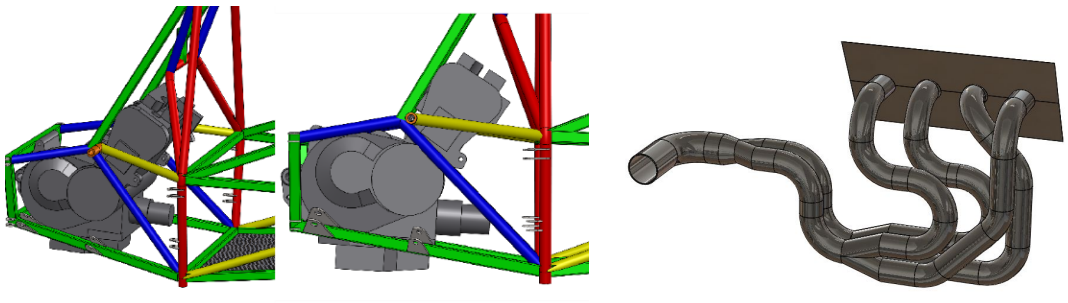

Figure 2. Space limitations and engine components (shown in left and middle images) restricted header design to the outlet wrapping around to the side of the chassis. As a result the design shown on the right was agreed upon. Cylinders 1-4 and 2-3 connect at the first collectors 20 inches in straight length from the cylinder head while the 1-4 and 2-3 pipes connect 10 inches downstream at the final collector.

Computational fluid modeling was experimented with using STAR CCM+ available through Portland State University. The flow model is simplified by incompressible, turbulent flow with velocity inlets and atmospheric pressure outlets. Figure 3 demonstrates the velocity vector field of the primary headers to the first collector using the previously explained model. The model contains smooth interior surfaces. The largest increase in flow velocity are located at the 180° bends where the largest curvature is found. However, despite the rudimentary methods used in the simulation, no further warrant for changes was found.

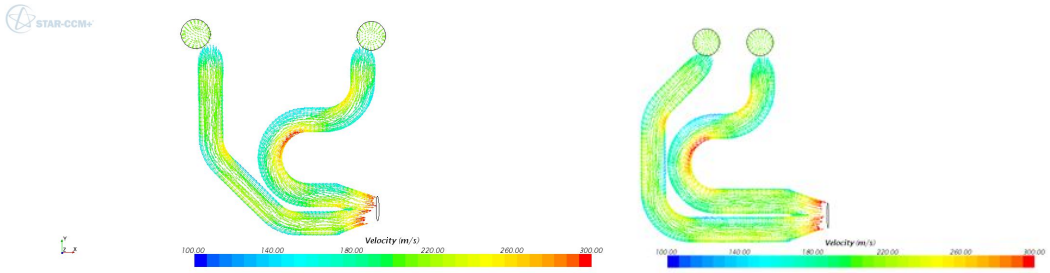

Figure 3. CFD simulation vector fields for inlet pipes 1 and 4 (left) and 2 and 3 (right). Current model assumes a 8149.61 in/s inlet velocity with an absolute outlet pressure of 1atm. Red spots represent increased velocities due to curved pipes.

IV. Muffler

Sound attenuation of an IC engine poses a unique challenge due to the noise spectrum variation and flow characteristics. A muffler must perform well at all engine speeds and therefore must be able to adequately attenuate sound across a range of frequencies. Exhaust system frequencies can vary between 50 and 4000 Hz (Sullivan 1978). Most exhaust noise is limited to the firing frequency and its first few harmonics. An equation given by Craig *et al.* (2012) gives the primary frequency at each engine speed by

$$f = \frac{RPM}{60}\frac{\#\,Pistons}{2} \tag{3}$$

where RPM is the engine speed and #Pistons is the number of pistons for the engine. For tabulated values of the eq. (3) see Appendix I.

There are two common approaches to the design of a muffler: absorptive and reflective. An absorptive muffler uses a sound absorbing material such as fiberglass or stainless steel wool, to convert acoustic energy into heat. Reflective mufflers induce a destructive wave interference in the exhaust stream to reduce the wave intensity. For complete destructive interference to occur a reflected pressure wave of equal amplitude that is 180^{o} out of phase needs to collide with the transmitted pressure wave (Potente 2005). A reflective muffler can be designed to pinpoint certain frequencies that are the primary contributors to exhaust noise while an absorptive muffler reduces intensity across a large frequency range.

The final muffler design is usually a combination of single sound attenuating elements that cohesively reduce the noise adequately over the full range of frequencies. A discussion of the unique single muffler elements follows.

Helmholtz resonator chambers

A Helmholtz resonator consists of an acoustic chamber that is branched off of the main header by a small diameter pipe. The neck of the resonator is analogous to a mass and the cavity to a spring similar to a mechanical spring-mass oscillator. As acoustic pressure waves encounter the resonator aperture, small amplitude oscillations of the fluid inside the neck act to dampen the wave and attenuate sound. The attenuation characteristics peak at a natural frequency of the system and, ideally, act as a stop-band filter. Real Helmholtz resonators often attenuate sound on the levels of 10 – 30 dB (Han 2008), depending on design and system parameters.

In application to a muffler, a Helmholtz resonator may be used to target specific frequencies of which either are the largest contributors to noise or are points at which other attenuating devices are ineffective. To do this, the geometry of the resonator may be designed

such that the frequency of interest matches the natural frequency of the resonator. Developed for low Mach numbers, Tang (2010) describes the natural frequency ω_o of a Helmholtz resonator

$$\omega_o = \sqrt{\frac{\rho_o C^2 A^2}{mV}} \tag{4}$$

where ρ_o is the density of the fluid in the resonator cavity, c is the speed of sound in the fluid, A is the cross-sectional area of the resonator neck, m is the effective mass in the resonator neck, and V is the resonator cavity volume. A general example of a helmholtz resonator can been seen in Fig. 4.

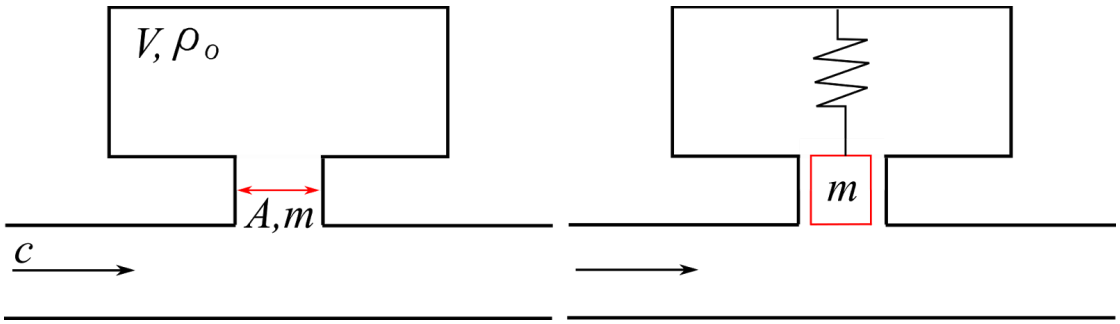

Figure 4. A Helmholtz type acoustic resonator with neck area A, effective mass m, cavity volume V, density ρ, and mean acoustic velocity c. Resonator simulates a spring mass damper where the cavity is analogous to a spring and neck to a mass.

Introduction of a mean flow to the pipe results in increased complexity. A pressure differential between the main pipe and resonator cavity can induce large amplitude oscillations, and if parameters are met such that the natural frequency of the system is encountered, noise can occur. To combat this, Tang (2010) experimented with two modifications to the resonator device. The first modification introduces a restriction to the neck cavity that increases damping forces at large amplitudes. The second modification involves connection of the main resonator cavity to an upstream location of the pipe flow by means of a small diameter tube. This minimizes the pressure differential that develops as pressure drops in the main pipe due to mass flow. Experiments conducted by Tang demonstrate the effectiveness of the Helmholtz resonator on sound attenuation. A baselines test with three flow rates and no-modifications to the resonator resulted in sound attenuations of around 12 dB with no mean flow and 315 in/s (8m/s) flow, and -20 dB at 472 in/s (12 m/s) and 709 in/s (18 m/s). Including modifications to the system resulted in sound attenuation of around 12 dB up to 472.44 in/s with less noise introduction at 709 in/s.

With the experiments by Tang (2010) and concepts of the Helmholtz resonator developed, the Helmholtz resonator was not chose as a standalone device due to its low sound

attenuation levels and range. With little obstruction to the flow and ease of frequency targeting this device was considered for use alongside other attenuating devices for the VMS muffler.

Perforated elements with interacting ducts

A solution for the sound attenuation of two concentric interacting ducts of diameter D1 and D2 and length L, as shown in Fig. 5, has been presented by Sullivan *et al.* (1978), and will be discussed in this section. The continuity and momentum equation can be solved as second-order, inhomogeneous differential equations with constant coefficients for control volume 1 and 2 as shown in Fig. 5. A solution by Eigenfunction expansion is presented by Sullivan *et al*. (1978). This solution satisfies the rigid wall boundary condition. Impedance of a perforated cylindrical chamber can be determined from experimental data presented by Sullivan *et al*. (1978). For a meaningful solution to be approached additional data must be collected or approximated for use as the inlet and outlet boundary conditions including inlet and outlet space average velocity and density. Solutions similar to that shown for perforated elements with two interacting ducts have been found for systems of three ducts with additional complexity.

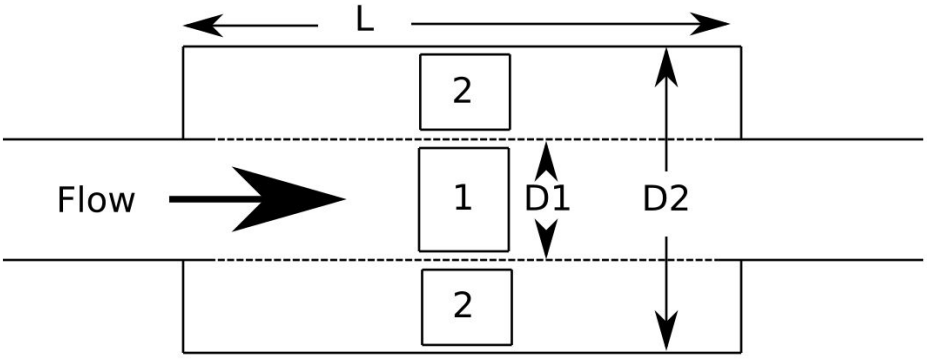

Figure 5. Control volumes is concentric-tube resonator.

Absorptive devices with perforated elements

An absorptive silencer reduces noise by transfer of pressure energy into heat energy. Acoustic pressure waves encounter materials with high absorption/low reflection properties often comprised of small, fibrous or porous spaces. A perforated tube allows mean flow of exhaust gases axially while pressure waves transmit radially into surrounding packing material. A descriptive analysis of an acoustically lined cylindrical “duct” is prohibitively complex. Fortunately, these types of mufflers are common, and experiments with various absorptive mufflers are relatively well researched. Potente (2015)

conducted an experiment with a Yoshimura RS-3 (Fig. 6) muffler with a 2.25 in. inner diameter and 4.5 in. outer diameter with an effective length of 18 in. Considerable sound attenuation was found across 11000 rpm, and almost sufficient muffling was found per FSAE rules, with the exception of one frequency at 125 Hz. With this test in mind, a muffler of similar dimensions but longer effective length is feasible with space on the VMS chassis.

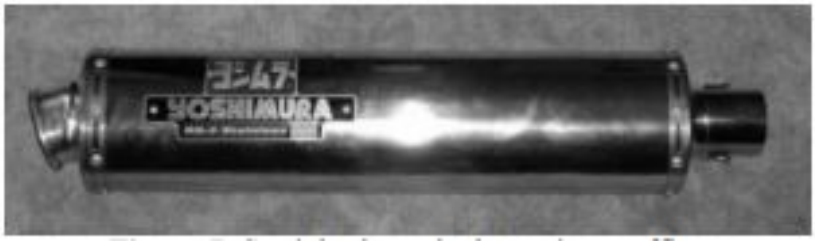

Figure 6. Yoshimura RS-3 muffler tested by Potente (2005) with inner diameter d = 2.25 in., outer diameter D = 4.5 in., and length L = 18 in. Noise tests resulted in sufficient attenuation for FSAE regulations with the exception of 125 Hz where the max decibel levels matched the highest value given by FSAE.

Final Design

The aforementioned muffler devices are just a small selection of the many types that are used in the industry. Consideration was made for each muffler depending on sound attenuating capabilities, confidence in effectiveness, ease of manufacturing, and limit in flow restrictions.

A combination of a Double-tuned resonator and Helmholtz resonator was initially suggested as it combines a simplistic design and long term effectiveness with elimination of maintenance or replacement of parts. However, due to necessary iterations as well as limit to sound attenuation levels, confidence in ability of the current team to manufacture the system in the allotted time was considerably low.

An absorptive muffler (see Fig. 7) was chosen for the final design in contrast to the resonator style muffler mentioned before. With a large frequency range for sound attenuation and little restriction to flow, the absorptive muffler was determined to be most practical for this project. Dimensions were chosen for two 14 in. channels in series for an effective 28 in. long attenuation chamber, increasing the muffler tested by Potente (2015) by 10 in. Full dimensions of the package are shown in Fig. 8.

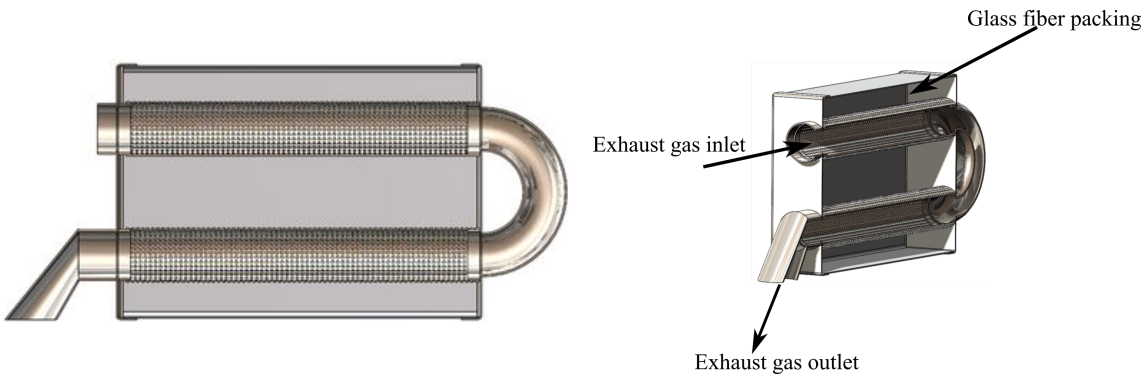

Figure 7. Muffler design incorporates a two chamber system with inlet at the top and outlet on the bottom. Fiber glass packing material was chosen as the absorptive material which fills in the muffler cavity around the inlet and outlet baffles.

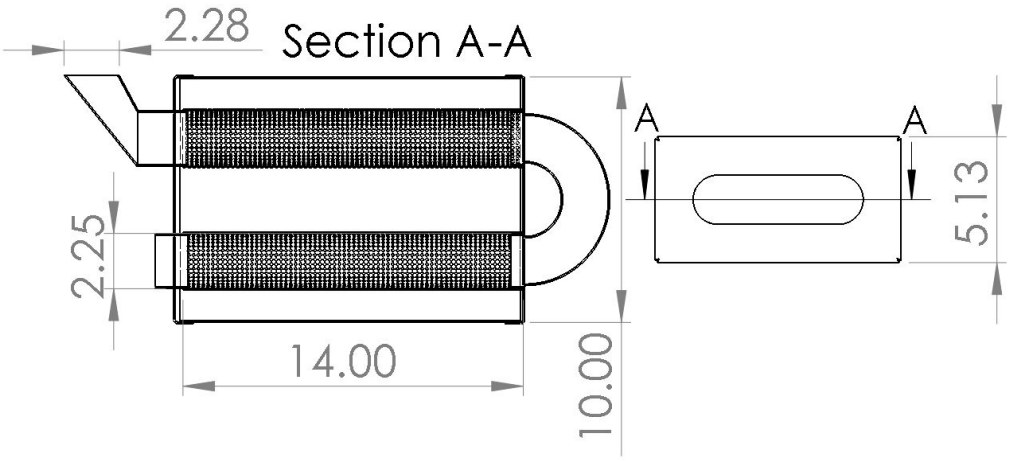

Figure 8. Specific dimensions include a 14x10x5in. Cavity with 2.25in. inlet and outlet pipes.

V. Materials

Header

For components related to the primary tubes connected to the engine block, high heat resistance and corrosion resistant were the main factors in material selection. Mild steel and stainless steels are common for their abilities to operate at high temperature conditions. Exhaust temperatures are on the order of 300 to 1000℉, with typical steel metals having melting temperatures at or exceeding 2600℉ (see Table 2). Ultimately, stainless steel was chosen for the final header material as it provides corrosion resistance characteristics.

Muffler

The muffler experiences lower gas temperature ranges than that of the header due to heat dissipation through the headers. Material selections pose opportunity to save on weight, a major design characteristic for performance cars. With a mild steel construction, the previous design weighed more than 12 lbs. With the expectation that the maximum temperature at the muffler will be on the order of 600℉, material selection is broadened to include those materials with lower melting temperatures. Choices include but were not limited to aluminum, steel, and carbon fiber. Aluminum and carbon fiber are considered more viable options for their weight reductions in comparison to steel, as seen in Table 2.

Table 2. Material properties.

Material	**Density kg/m^3**	**Melting Point °F**
Steel, Mild[1]	7850	2600-2800
Steel, Stainless[1]	7480-8000	2750
Aluminum[1]	2712	1220
*Carbon Fiber[2,3]	1600	6332
*Nomex(aramid)[4,5]	29	662
1 - Engineering Tool Box. 2 - Korshøjvej. (2006). 3 - Formula 1 - dictionary. 4 - Plascore, Inc. (2014). 5 - Encyclopædia Britannica *Properties estimated from multiple sources; real values may vary with manufacturer.		

Both aluminum and carbon fiber materials were pursued for the project. A small amount of carbon fiber and nomex composite material was donated through the PSAS teams; however, the resin used to bind the carbon fiber and nomex together had a glass transition temperature of approximately 300℉, well below the expected max temperature. High heat resin is available, but not within budget. An aluminum casing with stainless steel end caps was chosen for the final design. Stainless steel end-caps were chosen for manufacturing considerations.

VI. Manufacturing

Cutting and shaping

304 Stainless steel piping was sourced from a local company, *Columbia River Mandrel Bending* (see Fig. 9a). Sections were ordered in 180°, 45°, and 0° sections with enough material to manufacture headers with a few spare pieces for backup. In order to accurately cut 180° pieces to 90° elbows, an adjustable, acrylic cutting jig was manufactured, as seen in Fig. 9b. A vertical band saw was used to cut 90° elbows while straight pipes were cut to length on a horizontal band saw.

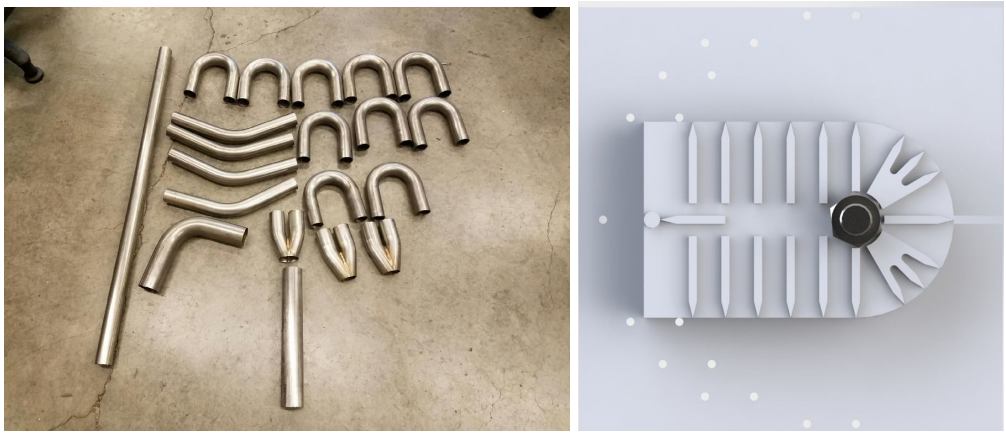

Figure 9. (Left) Raw 304 stainless steel pipes ordered from *Columbia River Mandrel Bending.* (Right) Cutting jig manufactured from acrylic plastic with adjustable center piece for 45° and 90° cuts

The header flange, muffler end plates, and muffler box-shell were outsourced to *Portland Waterjet* and bent to shape using a sheet metal brake. End plates were attached to the muffler box by means of rivets.

Welding

Tungsten Inert Gas (TIG) welding, chosen for pipe joining, is considered to be the superior to Metal Inert Gas (MIG) welding. Two important aspects of the TIG welding process are cleanliness and focused heat. Because of the inert environment provided by Argon gas-shielding used in the TIG welding process, the filler material can be an alloy of very similar properties to the parent material, creating a more homogenous weld. Adversely, MIG welding requires filler material with added detergents and cleaners to help create a similar homogenous weld. A second benefit of TIG welding is an increase in localized heat input which reduces the Heat-Affected Zone (HAZ). The HAZ is the region around the weld that has reduced mechanical strength due to heat input above the annealing temperature of the material. TIG welding causes a much smaller HAZ than MIG welding.

As a result of the previous discussion of welding methods, TIG welding was chosen for the joining process of all header pipe sections, flanges and joining surfaces.

VII. Results

The final design encompasses a few new features and aspects over the pre-existing design. First, an increase in pipe diameter from 1 in. to 1.5 in. was chosen by means of tabulated data regarding 4-stroke, 4-cylinder IC engines with a max operating engine speed of 8000 rpm. Second, equal pipe lengths were designed for all engine ports for a more equal power output from each cylinder. Related to this, the pipe lengths of 20 in. to first collector and 10 in. to secondary collector were chosen by means of estimating equations. These equations take into count cylinder bore, port diameter, stroke length, open valve period, and target engine speed. Next, the muffling method was chosen to be made of absorptive components. Absorptive mufflers combine low flow restrictions with sufficient cross range sound attenuation using a fairly simplistic design. An effective length of 28 in. was chosen with data from Potente (2005) and pre-existing muffler dimensions in mind. Upgrades to the muffler include removable end-plates for re-packing of muffling material as well as an aluminum case for weight considerations. The final design diminished weight by 2 lbs while increasing effective muffling capabilities.

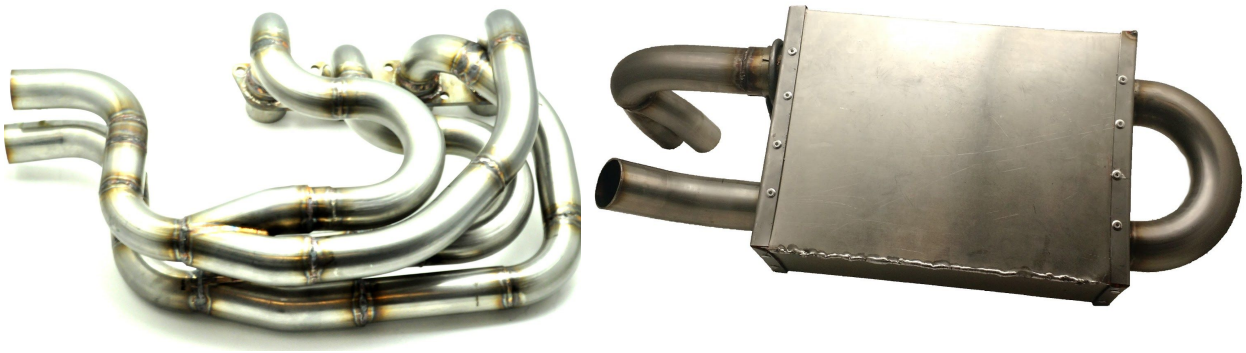

Figure 10. Completed 4-2-1 exhaust manifold (left) and absorptive muffler (right).

VIII. Testing

Preliminary indoor testing shows promising results, with peak readings of 94 dB at idle and 106 dB at max engine speed. Further testing outdoors resulted in 94 dB at idle and 104 dB at max engine speed. Dynamometer testing is scheduled for June 4th, at CorkSport Performance LLC for verification of performance characteristics. It is expected that the increase in header pipe diameter along with the equal length channels will provide equal power output from each cylinder and therefore better horsepower and torque curves. Finally, scale measurements of the new muffler shows a maintained weight of 10 lbs. Given the increase in overall dimensions to secure the noise attenuation performance of the new design, this maintained weight was found to be satisfactory to our sponsor as the new muffler not only meets FSAE regulations it also allows for maintenance and repacking by the VMS team when fibrous packing material becomes inoperable.

IX. Conclusion

The final muffler design incorporates design aspects for fluid and acoustic dynamics as well as material properties. Header dimensions were designed such that sufficient mass flow and gas velocity were optimal for a range of engine speeds while the muffler component was chosen to avoid flow restrictions while maintaining sufficient sound attenuation for competitions and events. The final manufactured header is made out of 304 stainless steel with diameter of 1.5 in. and total length of 30 in. The muffler is made of of aluminum and stainless steel with end-caps which can be removed for servicing/repacking. Sound tests show that the muffler attenuates sound below the limits of the FSAE regulations and scale measurements show a 2 lbs. improvement in muffler weight.

References

Bell, A. Graham. (1988) Performance Tuning in Theory and Practice: Four Strokes. Sparkford, Yeovil: Haynes. Print.

Carbon Fiber. (n.d.). Retrieved May 31, 2016, from http://www.formula1-dictionary.net/carbon_fiber.html

Korshøjvej. (2006). *Comfil Safety Data Sheet*. Denmark, Silkeborg.

Metals - Melting Temperatures. (n.d.). Retrieved May 31, 2016, from http://www.engineeringtoolbox.com/melting-temperature-metals-d_860.html

Plascore, Inc. (2014). *PN1 Commercial Grade Aramid Fiber Honeycomb*. Zeeland, MI.

Potente, D.. (2014). Design principles for an automotive muffler. *International Journal of Applied Engineering Research*.

Quattrochi, Douglas. (2006) "3.5 The Internal Combustion Engine (Otto Cycle)." 3.5 The Internal Combustion Engine (Otto Cycle). Web. 31 May 2016.

Smith, Philip Hubert, and John Cruikshank. Morrison. (1972) *The Scientific Design of Exhaust and Intake Systems*. R. Bentley. Cambridge, MA . Print.

Sullivan, J. (1978). Analysis of concentric-tube resonators having unpartitioned cavities. *J. Acoustic Soc. Am., 64*(1), 207-215.

STAR-CCM ® CFD Simulation Software. *STAR-CCM ® | CFD Simulation Software*. Web. 09 Mar. 2016. <http://www.cd-adapco.com/products/star-ccm®>.

The Editors of Encyclopædia Britannica. (n.d.). Aramid. Retrieved May 31, 2016, from http://www.britannica.com/science/aramid

Appendix.

Table 1. Primary Frequencies for eq. (3).	
RPM (revs/minute)	f (Hz)
2000	66.67
2500	83.33
3000	100.00
3500	116.67
4000	133.33
4500	150.00
5000	166.67
5500	183.33
6000	200.00
6500	216.67
7000	233.33
7500	250.00
8000	266.67
8500	283.33
9000	300.00
9500	316.67
10000	333.33
10500	350.00
11000	366.67
11500	383.33